

Quantitative determination of anisotropic magnetoelectric coupling in $\text{BiFeO}_3 - \text{CoFe}_2\text{O}_4$ nanostructures

Cite as: Appl. Phys. Lett. **97**, 052902 (2010); <https://doi.org/10.1063/1.3475420>

Submitted: 14 April 2010 . Accepted: 15 July 2010 . Published Online: 04 August 2010

Yoon Seok Oh, S. Crane, H. Zheng, Y. H. Chu, R. Ramesh, and Kee Hoon Kim



View Online



Export Citation

ARTICLES YOU MAY BE INTERESTED IN

Multiferroic magnetoelectric composites: Historical perspective, status, and future directions

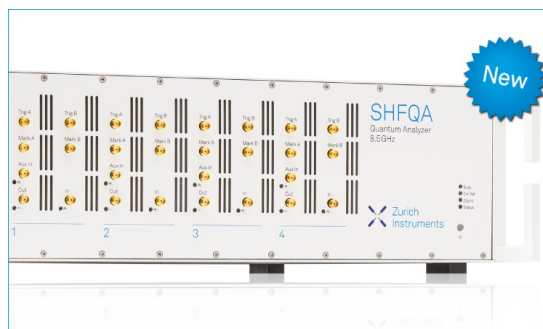
Journal of Applied Physics **103**, 031101 (2008); <https://doi.org/10.1063/1.2836410>

Direct measurement of magnetoelectric exchange in self-assembled epitaxial $\text{BiFeO}_3 - \text{CoFe}_2\text{O}_4$ nanocomposite thin films

Applied Physics Letters **94**, 192902 (2009); <https://doi.org/10.1063/1.3138138>

Magnetoelectric and multiferroic properties of variously oriented epitaxial $\text{BiFeO}_3 - \text{CoFe}_2\text{O}_4$ nanostructured thin films

Journal of Applied Physics **107**, 064106 (2010); <https://doi.org/10.1063/1.3359650>



Your Qubits. Measured.

Meet the next generation of quantum analyzers

- Readout for up to 64 qubits
- Operation at up to 8.5 GHz, mixer-calibration-free
- Signal optimization with minimal latency

Find out more



Quantitative determination of anisotropic magnetoelectric coupling in $\text{BiFeO}_3\text{-CoFe}_2\text{O}_4$ nanostructures

Yoon Seok Oh,¹ S. Crane,² H. Zheng,² Y. H. Chu,³ R. Ramesh,² and Kee Hoon Kim^{1,a)}

¹*CeNSCMR, Department of Physics and Astronomy, Seoul National University, Seoul 151-747, Republic of Korea*

²*Department of Materials Science and Engineering, University of California, Berkeley, California 94720, USA*

³*Department of Materials Science and Engineering, National Chiao Tung University, HsinChu 30010, Taiwan*

(Received 14 April 2010; accepted 15 July 2010; published online 4 August 2010)

The transverse and longitudinal magnetoelectric susceptibilities (MES) were quantitatively determined for (001) heteroepitaxial $\text{BiFeO}_3\text{-CoFe}_2\text{O}_4$ nanostructures. Both of these MES values were sharply enhanced at magnetic fields below 6 kOe and revealed asymmetric line shapes with respect to the dc magnetic field, demonstrating the strain-induced magnetoelectric effect. The maximum transverse MES, which reached as high as ~ 60 mV/cm Oe, was about five times larger than the longitudinal MES. This observation signifies that transverse magnetostriction of the CoFe_2O_4 nanopillars is enhanced more than the bulk value due to preferred magnetic domain alignment along the [001] direction coming from compressive, heteroepitaxial strain. © 2010 American Institute of Physics. [doi:10.1063/1.3475420]

The magnetoelectric (ME) effect is a physical phenomenon in which the electric polarization P (magnetization M) is modulated by the magnetic field H (electric field E). There is a growing interest in the application of ME effects toward various devices, including magnetic sensors¹ and energy harvesters.² As such, numerous efforts have been made to obtain strong ME couplings in ME composites made of ferroelectric (or piezoelectric) and ferromagnetic materials.^{3,4} In these types of ME composites, P is varied with M via the strain (u)-coupling at the interface between the piezoelectric and magnetostrictive phases. Thus, the configuration of this interface is a significant control parameter for determining the extent of ME coupling.¹ In this respect, a layered sandwich structure [i.e., (2–2) structures] produces a larger ME coupling than for particulates that are dispersed in a matrix [i.e., (0–3) structures] because the former has a larger interface area. In contrast, this common practice cannot be applied to multilayered thin films, where clamping of the non-magnetic substrate can prevent strain-coupling between the layers.⁵

In 2004, an epitaxial thin film composed of CoFe_2O_4 (CFO) nanopillars embedded in a BaTiO_3 (BTO) matrix [i.e., (1–3) structures] was grown and suggested to be an alternative to circumvent the substrate clamping effect. On the other hand, it has been quite difficult to determine quantitatively the ME coupling of such nanostructures and, more generally, numerous ME films, except observing the existence of non-trivial ME coupling.⁶ One dominant reason for this difficulty is that the ME voltage signal is proportional to the film thickness; it typically becomes smaller than 1 μV for film thicknesses less than 1 μm . To overcome this difficulty, a large ac magnetic field (H_{ac}) of up to ~ 1 kOe was recently used to obtain the effective MES as a function of H_{ac} .^{7,8} However, direct measurements of the MES based on a conventional scheme that employs small H_{ac} values with variations in the

dc magnetic field (H_{dc}) would be useful for understanding the ME coupling of numerous multiferroic films or nanostructures at the quantitative level. In this work, by use of the conventional scheme, we provide experimental evidences that a 300 nm thick $\text{BiFeO}_3\text{-CoFe}_2\text{O}_4$ (BFO–CFO) nanostructure has a peculiar MES anisotropy that is not expected in bulk forms of those materials.

The self-assembled epitaxial BFO–CFO film with thickness of 300 nm was grown on a (001) $\text{SrRuO}_3/\text{SrTiO}_3$ substrate by pulsed laser deposition.⁹ The film had the CFO nanopillars embedded in a BFO matrix with a volume fraction of 1:1. Top electrodes Pt/ SrRuO_3 were deposited on the film surface [Fig. 1(a)]. For magnetic hysteresis measurements, a vibrating sample magnetometer was utilized. For ferroelectric hysteresis loops, the displacement current was measured using a fast digitizer and a high voltage amplifier.

To investigate the MES ($\alpha \equiv \delta P / \delta H_{ac}$), especially for thin films, we developed a highly sensitive ME susceptometer that operates inside the PPMs (Quantum Design). A pair of solenoids was designed to induce a H_{ac} of ~ 4 Oe inside the solenoid pair and a voltage pick-up coil was used to determine the phase of H_{ac} . In particular, modulated charges, instead of voltages, were measured using a high-impedance

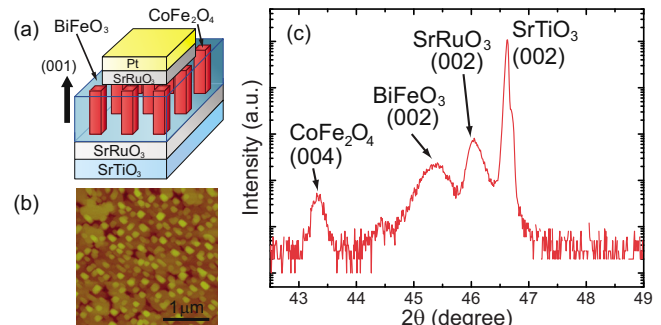


FIG. 1. (Color online) (a) Schematic picture, (b) AFM image, and (c) XRD pattern of the BFO–CFO film with nanopillar structures.

^{a)}Electronic mail: khkim@phya.snu.ac.kr.

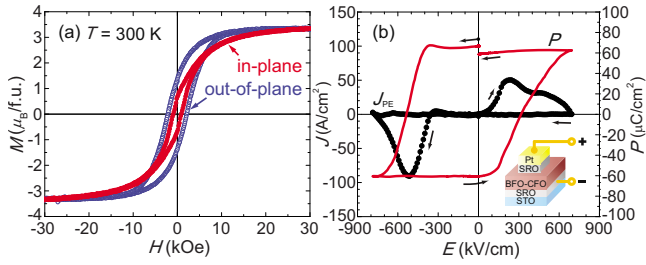


FIG. 2. (Color online) (a) Magnetic hysteresis loops for the in-plane and out-of-plane directions measured at 300 K. M is normalized to the volume fraction of CFO. (b) $J_{PE}(E)$ (solid circle) was integrated to estimate the P - E hysteresis loop (solid line).

charge amplifier with a gain factor of 10^{12} V/C. This makes the amplified signal independent of film thickness but proportional to electrode area so that the signal-to-noise ratio was improved. Based on this scheme, we were able to detect small ME charges in a thin film with a thickness ~ 40 nm and a circular electrode of diameter ~ 100 μm . The lowest charge noise (ΔQ) was $\sim 10^{-17}$ C, which corresponded to a voltage noise of $\Delta Q/C_s$ (C_s =sample capacitance). The determined α could be converted into the MES expressed as a voltage unit $\alpha_E = \delta E / \delta H_{ac}$ using the relationship $\alpha = \varepsilon \alpha_E$, where ε is the absolute permittivity of a specimen.

Figure 1(b) shows an atomic force microscopy (AFM) image of the BFO-CFO film, in which the CFO phase appears as rectangles embedded in the BFO matrix.⁹ Fig. 1(c) further shows an x-ray diffraction (XRD) pattern of the film obtained through a θ - 2θ scan around the (002) SrTiO₃ peak. The distinct (00 l) peaks of CFO, BFO, and SrRuO₃ are consistent with the previous result⁹ that each phase was epitaxially grown on the SrTiO₃ substrate. The d -spacing of the CFO nanopillars was estimated as 2.0867 Å from the (004) peak. This indicates a compressive strain along the [001] direction, $u_{001} = -0.33\%$, compared with the bulk CFO. Figure 2(a) shows the magnetic hysteresis loops measured along the in-plane (i.e., $H \parallel [100]$) and out-of-plane (i.e., $H \parallel [001]$) directions. The saturated moment of ~ 3.4 $\mu_B/\text{f.u.}$ for both directions was in good agreement with the reported CFO value.¹⁰ Moreover, there existed a large uniaxial magnetic anisotropy with an easy axis along the [001] direction. A linear extrapolation of the in-plane loop yielded a magnetic anisotropy field of ~ 25 kOe. In a previous study on BTO-CFO nanostructures, the compressive strain of CFO caused by heteroepitaxial growth was found to be a primary contribution to the uniaxial magnetic anisotropy;¹¹ a large magnetic anisotropy field of 51 kOe was observed for $u_{001} = -1.1\%$, while the anisotropy field decreased for smaller u_{001} . Therefore, even in the BFO-CFO film studied here, the magnetic anisotropy field of ~ 25 kOe seems to originate from the presence of a compressive, heteroepitaxial strain of $u_{001} = -0.33\%$ inside the CFO nanopillars.

To determine the P - E loop, displacement current $J(E)$ was measured while negative, positive, and zero biases were applied successively in sequence (i.e., $-E$ to E to 0). The $J(E)$ curve showed two extremes at -500 kV/cm and 200 kV/cm, at which a reversal of P occurred. In addition to these extremes, a nonlinear background was found in the $J(E)$ curve. This could have been from either a Schottky barrier at the interface or a ferroelectric diode effect.^{12,13} After subtracting the nonlinear background, the remaining

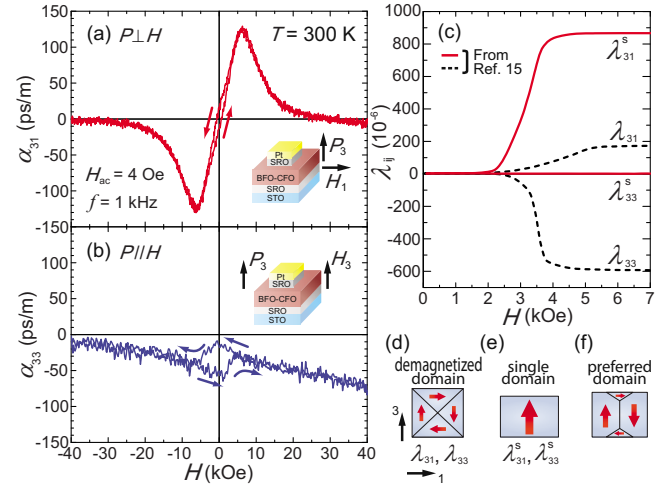


FIG. 3. (Color online) (a) Transverse (α_{31}) and (b) longitudinal MES (α_{33}) of the BFO-CFO nanostructure at 300 K. (c) Dashed (solid) lines represent the transverse (λ_{31}) and longitudinal (λ_{33}) magnetostriction curves of a $\text{Co}_{0.8}\text{Fe}_{2.2}\text{O}_4$ crystal with the demagnetized (single) magnetic domain. (d) Demagnetized, (e) single, and (f) preferred magnetic domain patterns of CFO are schematically drawn.

current density $J_{PE}(E)$ was integrated. In the obtained P - E loop [Fig. 2(b)], the polarization value was normalized by the volume fraction of BFO. The saturated $P(P_s)$ of ~ 62 $\mu\text{C}/\text{cm}^2$ is comparable to the previously obtained value in an epitaxial (001) BFO film.¹⁴ After fully poling the sample along the positive P direction, i.e., top electrode direction as indicated in the inset of Fig. 2(b), all the MES measurements were subsequently performed.

Figure 3 summarizes transverse (α_{31}) and longitudinal (α_{33}) MES curves as a function of H_{dc} . We note that the similar α_{31} and α_{33} curves were obtained at many different electrode spots of the same film and at those of the same kind of nanostructured film with a thickness ~ 40 nm. The α_{31} clearly shows a sign reversal with the direction of H_{dc} and develops extreme points at $H_{dc} = \mp 6$ kOe. This is the archetypal line shape expected in the strain-coupled ME media composed of piezoelectric and magnetostrictive materials, supporting that the measured MES data are reliable. In addition, the α_{33} curve exhibited an asymmetric line shape with H_{dc} , which was similar to the case of α_{31} . However, in this α_{33} curve, a small but non-negligible offset at $H_{dc} = 0$ was observed, of which value was proportional to the electrode area. Thus, this offset was attributed to a small contribution from eddy currents generated inside the electrode due to δH_{ac} . Except for this offset, the α_{33} curve was almost an odd function of H_{dc} . This further supports that the strain-coupling is a dominant source of the longitudinal ME effect as well.

As shown in Fig. 3, $\alpha_{31} > 0$ for $H_{dc} > 0$ while $\alpha_{33} < 0$ for $H_{dc} > 0$. This experimental result reflects that P_3 (i.e., $P \parallel [001]$) increases under $H_{dc} \parallel [100]$, while P_3 decreases under $H_{dc} \parallel [001]$. When the $H_{dc} \parallel [100]$ was applied to the CFO crystal, the transverse magnetostriction (λ_{31}) was positive [dashed lines in Fig. 3(c)]. Thus, the CFO nanopillars and the BFO matrix, via strain-coupling, were expected to be elongated along the [001] direction.¹⁵ It is known from an earlier study that P_3 increases due to the rotation of P with increasing length along the [001] direction.^{16,17} Therefore, the observation of $\alpha_{31} > 0$ for $H_{dc} > 0$ can be qualitatively under-

stood as the result of an elongation of CFO/BFO along the [001] direction under $H_{dc} \parallel [100]$ and the subsequent increase in P_3 . The case of decreasing P_3 under $H_{dc} \parallel [001]$ can also be understood in a similar way because the longitudinal magnetostriction (λ_{33}) in the CFO crystal was negative.

However, our MES data are seemingly inconsistent with the magnetostriction behavior of a bulk CFO at the quantitative level. The maximum to minimum value of $\alpha_{31}(\Delta\alpha_{31})$ in Fig. 3(a), amounting to ~ 260 ps/m (~ 120 mV/cm Oe), is about five times larger than that of $\alpha_{33}(\Delta\alpha_{33})$. According to the magnetostriction of a $\text{Co}_{0.8}\text{Fe}_{2.2}\text{O}_4$ crystal with demagnetized domains [Fig. 3(c)], a slope of the λ_{33} versus H curve is at least twice that of the λ_{31} versus H curve.¹⁵ Upon assuming that the magnetostriction of CFO nanopillars follows a bulk behavior, these magnetostriction data predict that $\Delta\alpha_{33}$ should be at least twice of $\Delta\alpha_{31}$, which is in sharp contrast with the results in Figs. 3(a) and 3(b).

Although there might exist several mechanisms to induce enhanced α_{31} as discussed in a recent anisotropic MES study using large H_{ac} ,⁸ one most decisive factor could be the preferred magnetic domains existing in the CFO nanopillars. The solid lines in Fig. 3(c) reproduce published λ_{31}^s and λ_{33}^s for a $\text{Co}_{0.8}\text{Fe}_{2.2}\text{O}_4$ crystal with a single magnetic domain along the [001] direction. The single magnetic domain was obtained through the magnetic annealing process, i.e., cooling under H from high to room temperature.¹⁵ In this situation, applied $H \parallel [001]$ gave rise to the 180° domain wall motion, which resulted in negligible λ_{33}^s . In contrast, $H \parallel [100]$ resulted in a 90° domain wall motion so that it produced quite large λ_{31}^s . As we discussed above, the compressive, heteroepitaxial strain was a main source of enhanced magnetic anisotropy along the [001] direction in the CFO nanopillars. It is thus likely that the magnetic domains inside the CFO nanopillars have preferred alignment along the [001] direction, as illustrated in Fig. 3(f). If so, similar to the case of single magnetic domains, the CFO nanopillars are expected to have enhanced λ_{31} and suppressed λ_{33} . As a result, as observed in Figs. 3(a) and 3(b), the BFO–CFO nanostructure will give rise to a bigger α_{31} (smaller α_{33}) than that expected based on the behavior of bulk CFO magnetostriction.

These results point to the possibility that the strain-induced ME coupling in the nanostructured film can be quite different from the macroscopic bulk composite. Application of a compressive, heteroepitaxial strain to the CFO nanopillars enables to achieve increased α_{31} to as high as ~ 130 ps/m (~ 60 mV/cm Oe) at 6 kOe. Upon increasing $|u_{001}|$, as done in the BTO–CFO nanostructures with growth temperatures,¹¹ the α_{31} can be further optimized. In comparison, our previous study on a thin film made of NiFe_2O_4 nanoparticles embedded in a $\text{PbZr}_{0.52}\text{Ti}_{0.48}\text{O}_3$ matrix, [i.e., the (0–3) structure] showed maximum $|\alpha_{31}| = 4$ mV/cm Oe (~ 4 ps/m) and $|\alpha_{33}| = 16$ mV/cm Oe (~ 14 ps/m),¹⁸ which was clearly smaller than the maximum $\alpha_{31} \sim 130$ ps/m found here. Therefore, our results strongly support that thin films with the (1–3) nanostructure have larger ME couplings

than the other nanostructures [e.g., (0–3) structure].

In conclusion, we have determined the anisotropic MES of a 300 nm thick BiFeO_3 – CoFe_2O_4 nanostructure. An enhancement was observed in the transverse configuration, which can be explained by the preferred alignment of magnetic domain resulting from the heteroepitaxial strain that is unique to the present (1–3) nanostructure. This investigation offers quantitative evidences that the nanoscale engineering of strain coupling is useful for the design of ME devices.

We appreciate discussions with T. W. Noh. This study was supported by the NRF, Korea through National Creative Research Initiatives, NRL (Grant No. M10600000238) and Basic Science Research (Grant No. 2009-0083512) programs and by MOKE through the Fundamental R&D Program for Core Technology of Materials. Y.S.O. is supported by Seoul R&BD (Grant No. 10543). Y.H.C. is supported by the National Science Council, R.O.C. (Grant No. NSC 98-2119-M-009-M016).

¹C. W. Nan, M. I. Bichurin, S. X. Dong, D. Viehland, and G. Srinivasan, *J. Appl. Phys.* **103**, 031101 (2008).

²S. X. Dong, J. Y. Zhai, J. F. Li, D. Viehland, and S. Priya, *Appl. Phys. Lett.* **93**, 103511 (2008).

³J. Van den Boomgaard, A. M. J. G. Van Run, and J. Van Suchtelen, *Ferroelectrics* **14**, 727 (1976).

⁴J. Ryu, A. V. Carazo, K. Uchino, and H. E. Kim, *J. Electroceram.* **7**, 17 (2001).

⁵C. W. Nan, G. Liu, Y. H. Lin, and H. D. Chen, *Phys. Rev. Lett.* **94**, 197203 (2005).

⁶H. Zheng, J. Wang, S. E. Lofland, Z. Ma, L. Mohaddes-Ardabili, T. Zhao, L. Salamanca-Riba, S. R. Shinde, S. B. Ogale, F. Bai, D. Viehland, Y. Jia, D. G. Schlom, M. Wuttig, A. Roytburd, and R. Ramesh, *Science* **303**, 661 (2004).

⁷L. Yan, Z. P. Xing, Z. G. Wang, T. Wang, G. Y. Lei, J. F. Li, and D. Viehland, *Appl. Phys. Lett.* **94**, 192902 (2009).

⁸L. Yan, Z. G. Wang, Z. P. Xing, J. F. Li, and D. Viehland, *J. Appl. Phys.* **107**, 064106 (2010).

⁹H. M. Zheng, F. Straub, Q. Zhan, P. L. Yang, W. K. Hsieh, F. Zavaliche, Y. H. Chu, U. Dahmen, and R. Ramesh, *Adv. Mater. (Weinheim, Ger.)* **18**, 2747 (2006).

¹⁰R. Pauthenet, *Compt. Rend.* **230**, 1842 (1950).

¹¹H. M. Zheng, J. Kreisel, Y. H. Chu, R. Ramesh, and L. Salamanca-Riba, *Appl. Phys. Lett.* **90**, 113113 (2007).

¹²T. Choi, S. Lee, Y. J. Choi, V. Kiryukhin, and S. W. Cheong, *Science* **324**, 63 (2009).

¹³C. H. Yang, J. Seidel, S. Y. Kim, P. B. Rossen, P. Yu, M. Gajek, Y. H. Chu, L. W. Martin, M. B. Holcomb, Q. He, P. Maksymovych, N. Balke, S. V. Kalinin, A. P. Baddorf, S. R. Basu, M. L. Scullin, and R. Ramesh, *Nature Mater.* **8**, 485 (2009).

¹⁴J. Wang, J. B. Neaton, H. Zheng, V. Nagarajan, S. B. Ogale, B. Liu, D. Viehland, V. Vaithyanathan, D. G. Schlom, U. V. Waghmare, N. A. Spaldin, K. M. Rabe, M. Wuttig, and R. Ramesh, *Science* **299**, 1719 (2003).

¹⁵R. M. Bozorth, E. F. Tilden, and A. J. Williams, *Phys. Rev.* **99**, 1788 (1955).

¹⁶C. Ederer and N. A. Spaldin, *Phys. Rev. Lett.* **95**, 257601 (2005).

¹⁷H. W. Jang, S. H. Baek, D. Ortiz, C. M. Folkman, R. R. Das, Y. H. Chu, P. Shafer, J. X. Zhang, S. Choudhury, V. Vaithyanathan, Y. B. Chen, D. A. Felker, M. D. Biegalski, M. S. Rzchowski, X. Q. Pan, D. G. Schlom, L. Q. Chen, R. Ramesh, and C. B. Eom, *Phys. Rev. Lett.* **101**, 107602 (2008).

¹⁸H. Ryu, P. Murugavel, J. H. Lee, S. C. Chae, T. W. Noh, Y. S. Oh, H. J. Kim, K. H. Kim, J. H. Jang, M. Kim, C. Bae, and J. G. Park, *Appl. Phys. Lett.* **89**, 102907 (2006).